J. Fluid Mech. (2008), *vol.* 608, *pp.* 319–336.
doi:10.1017/S0022112008002152 Printed in the United Kingdom

Time-dependent force acting on a particle moving arbitrarily in a rotating flow, at small Reynolds and Taylor numbers

FABIEN CANDELIER

GEPEA – UMR UMR 6144, Ecole des Mines de Nantes – La Chantrerie, 4 rue Alfred Kastler, BP 20722, 44 307 Nantes, France

(Received 19 November 2007 and in revised form 24 April 2008)

The arbitrary motion of a solid sphere released in a solid-body rotating fluid is investigated theoretically in the limit of small Reynolds and Taylor numbers. The angular velocity of the fluid is assumed to be constant and under the premise that $Ta^{1/2} \gg Re$, the simplicity of the unperturbed flow enables us to calculate analytically the force acting on a particle moving with a harmonic slip velocity (by means of matched asymptotic expansions), when both inertia and unsteady effects are taken into account. Subsequently, these single-frequency results are used in order to determine the temporal expression of the force acting on an arbitrarily moving sphere, since the problem under study is linear. This force is first determined in a co-rotating reference frame and takes the form of two convolution products involving the particle acceleration and the particle velocity. For convenience, the corresponding expression of this force is also derived in the laboratory reference frame, and the particle motion equation obtained is thereafter illustrated by dealing with two practical situations, where unsteady and inertia effects must be taken into account to predict the particle dynamics accurately.

1. Introduction

This paper considers the motion of a spherical particle moving in a rigidly rotating fluid. The determination of the force experienced by a particle in such a case has been a challenge for several decades. This problem has many fundamental aspects with obvious applications (i.e. centrifuges). For later convenience, we should specify now that in a rotating reference frame, with an angular velocity of $\omega_0 \boldsymbol{e}_3$, the particle motion equation can be written as

$$m_p \frac{\mathrm{d}\boldsymbol{v}_p}{\mathrm{d}t} = m_p \boldsymbol{g} - m_p \omega_0^2 \boldsymbol{e}_3 \times (\boldsymbol{e}_3 \times \boldsymbol{x}_p) - 2m_p \omega_0 \boldsymbol{e}_3 \times \boldsymbol{v}_p + \boldsymbol{F} \tag{1.1}$$

where m_p is the particle mass, $\boldsymbol{x}_p$ and $\boldsymbol{v}_p$ are, respectively, the particle position and velocity (relative to the rotating reference frame) and $\boldsymbol{F}$ corresponds to the hydrodynamic force experienced by the particle. Note that such a reference frame is not Galilean, therefore a centrifugal force and a Coriolis force, respectively given by the second and third terms on the right-hand side of (1.1), must be taken into account in the particle motion equation. Following the classical approach, the hydrodynamic force is generally split in two parts: $\boldsymbol{F} = \boldsymbol{F}^0 + \boldsymbol{F}^1$, where $\boldsymbol{F}^0$ is the force due to the unperturbed flow, and $\boldsymbol{F}^1$ is the force corresponding to the induced (perturbation) flow. In the particular case of a rigidly rotating fluid, the unperturbed velocity is null

if it is expressed in a co-rotating reference frame, and therefore $\boldsymbol{F}^0$ comes only from the unperturbed pressure field. By using the gradient theorem, we can check that

$$\boldsymbol{F}^0 = \int_{\mathscr{V}} -\nabla P^0 \, \mathrm{d}\mathscr{V} = -m_f \left(\boldsymbol{g} - \omega_0^2 \boldsymbol{e}_3 \times (\boldsymbol{e}_3 \times \boldsymbol{x}_p) \right), \tag{1.2}$$

where $\mathscr{V}$ is the particle volume, and m_f is the fluid mass within the particle, and the particle motion equation can be recast in the form:

$$m_p \frac{\mathrm{d}\boldsymbol{v}_p}{\mathrm{d}t} = (m_p - m_f)\left(\boldsymbol{g} - \omega_0^2 \boldsymbol{e}_3 \times (\boldsymbol{e}_3 \times \boldsymbol{x}_p) \right) - 2 m_p \omega_0 \boldsymbol{e_3} \times \boldsymbol{v}_p + \boldsymbol{F}^1(t). \tag{1.3}$$

Obviously, the main difficulty lies in the determination of $\boldsymbol{F}^1$, the analytical expression of which has been derived only in a few particular situations.

In this connection, we should first mention the seminal article of Childress (1964), who addressed the problem of a sphere moving steadily along the rotation axis. He was one of the first to use matched asymptotic expansions in order to determine the fluid inertia contribution to the drag acting on a particle immersed in a non-uniform flow. In the limit of $1 \gg Ta^{1/2} \gg Re$, where $Ta = a^2\omega_0/\nu$ is the Taylor number (a is the radius of the sphere and ν is the fluid kinematical viscosity) and $Re = a|\boldsymbol{v}_p|/\nu$ is the particle Reynolds number, he found that

$$\boldsymbol{F}^1 = -6\pi\mu a \left(1 + \tfrac{4}{7} Ta^{1/2}\right) \boldsymbol{v}_p, \tag{1.4}$$

which was carefully checked experimentally by Maxworthy (1965).

Childress' result was generalized by Herron, Davis & Bretherton (1975) to a more complex case, corresponding to the three-dimensional motion of a particle within a vertical centrifuge (i.e. co-aligned with gravity). Note that in the problems addressed by Childress (1964), and by Herron *et al.* (1975), it turns out that the induced-flow equations, which are written in a co-rotating reference frame linked to the particle's centre, degenerate into quasi-steady equations, owing to the velocity naturally adopted by the particle. Moreover, convective effects are rendered negligible owing to the order of the Taylor and the Reynolds numbers, so that the near field is dominated by Stokes flow, while the far field is perturbed by a viscously modified Taylor column, owing to Coriolis acceleration (see again Herron *et al.* 1975). This far field induces modifications in the near field, and the classical force obtained in the creeping flow limit must be corrected accordingly. This force reads

$$\boldsymbol{F}^1 = -6\pi\mu a \left(1 + \sqrt{Ta} \begin{pmatrix} M_{11} & -M_{12} & 0 \\ M_{12} & M_{11} & 0 \\ 0 & 0 & M_{33} \end{pmatrix} \right) \cdot \boldsymbol{v}_p, \tag{1.5}$$

where $M_{11} = 5/7$, $M_{12} = 3/5$ and $M_{33} = 4/7$, and these results were checked experimentally by Candelier, Angilella & Souhar (2005) for solid and gaseous inclusions.

Another result to note corresponds to the case of a particle held fixed in the laboratory reference frame with the conditions $1 \gg Ta^{1/2} \gg Re$ still fulfilled. In such a case, the induced-flow equations are now steady, if they are written in a fixed reference frame linked to the particle centre, but the far field is perturbed by convective effects, which have to be taken into account in order to predict accurately the force acting on the sphere. The corresponding force was first derived by Gotoh (1990), and its analytical expression reads almost like (1.5), except that coefficients M_{11} and M_{12} must

be replaced by

$$M_{11} = \frac{3\sqrt{2}}{280}(19 + 9\sqrt{3}), \quad M_{12} = \frac{3\sqrt{2}}{280}(19 - 9\sqrt{3}), \tag{1.6}$$

and $\boldsymbol{v}_p$ must be replaced by the particle's slip velocity relative to the laboratory reference frame. (Note that these coefficients were derived for $\omega_0 > 0$, and we can check that if the rotation direction is reverse, then the sign of M_{12} changes accordingly.) Gotoh's results show that the lift force acting on the sphere is centripetal (see for instance the experiments of van Nierop *et al.* 2007), in contrast to the lift force that would be obtained by using an empirical force based on Saffman's (1965) results. His results therefore invalidate the systematic use of an additive Saffman lift force when the flow under study is not a pure shear flow.

Let us insist on the fact that so far, all the results presented were derived after assuming that the induced-flow equations were steady, according to the reference frame used. When the induced-flow equations are also unsteady, the difficulty in obtaining the force acting on the particle increases significantly since both unsteady and inertia effects contribute to the particle drag and lift forces in a complex and non-additive manner (see for instance the analytical investigation of Candelier & Angilella 2006). This is the reason why analytical determinations of the force experienced by a particle moving unsteadily in a non-uniform flow are still scarce, and results on this topic are generally quite recent. For instance, we can refer to the pioneering work of Miyazaki *et al.* (1995), or a few years later, to that of Asmolov & McLaughlin (1999) (see also Candelier & Souhar 2007) who addressed the problem of a sphere moving with a harmonic slip velocity in a shear flow. Concerning rotating flow, Miyazaki (1995) has also solved the problem of a sphere moving with a harmonic velocity (i.e. $\boldsymbol{v}_p = \boldsymbol{v}\exp(-\mathrm{i}\omega t)$), relative to the co-rotating reference frame. In the limit of weak unsteadiness ($a^2\omega/\nu \ll 1$) where ω is the angular frequency of the particle velocity, Miyazaki obtained

$$\boldsymbol{F}^1 = -6\pi\mu a \left(1 + \sqrt{Ta}\begin{pmatrix} f(\Omega) & -g(\Omega) & 0 \\ g(\Omega) & f(\Omega) & 0 \\ 0 & 0 & h(\Omega) \end{pmatrix}\right) \cdot \boldsymbol{v}_p, \tag{1.7}$$

where

$$f = (1/140)(\sqrt{-\mathrm{i}(2+\Omega)^3}(25 - 3\Omega + \Omega^2) + \sqrt{\mathrm{i}(2-\Omega)^3}(25 + 3\Omega + \Omega^2)), \tag{1.8}$$

$$g = -(\mathrm{i}/20)(\sqrt{-\mathrm{i}(2+\Omega)^3}(-3 + \Omega) + \sqrt{\mathrm{i}(2-\Omega)^3}(3 + \Omega)), \tag{1.9}$$

$$h = (1/70)(\sqrt{-\mathrm{i}(2+\Omega)^3}(10 + 3\Omega - \Omega^2) + \sqrt{\mathrm{i}(2-\Omega)^3}(10 - 3\Omega - \Omega^2)). \tag{1.10}$$

and where $\Omega = \omega/\omega_0$ is the normalized angular frequency. His results are in agreement with those of Herron *et al.* (1975) in the steady case limit ($\Omega \to 0$), but unfortunately, and if we are not mistaken, we do not recover $f(\Omega) \sim h(\Omega) \sim \sqrt{-\mathrm{i}\Omega}$ and $g(\Omega) \to 0$, when $\Omega \gg 1$, in contrast to Miyazaki's statements. (This is probably due to a minor typographic error.)

The present study seeks to gather together all the results mentioned in this introduction, by carrying out the analytical expression of the force acting on a particle in the limit of

$$1 \gg Ta^{1/2} \gg Re, \tag{1.11}$$

regardless of the particle's velocity. Such a result could therefore be used in many practical situations where the motion of a particle is inherently unsteady. For instance,

this is the case if a particle moves in a horizontal rotating flow (see for example the experiments of van Nierop *et al.* 2007).

Note that because the single-frequency results published by Miyazaki (1995) seem to be incorrect when $\Omega \gg 1$, and because they are involved in the calculation of the force acting on an arbitrarily moving particle, we will first be led, in what follows, to re-establish such results. This will be done, however, by using a different formalism.

2. Force $\boldsymbol{F}^1$ for the oscillating motion of a particle

In order to derive the force acting on a particle immersed in such a flow, it is convenient to work in a reference frame which also rotates at the same angular velocity as the fluid, but which is now moving with the particle, so that the fluid velocity $\boldsymbol{w}(\boldsymbol{x}, t)$ is therefore measured relative to the bulk flow and the velocity of the particle. In such a reference frame, the fluid motion equations are

$$\nabla \cdot \boldsymbol{w} = 0, \tag{2.1}$$

$$\rho\left(\frac{\partial \boldsymbol{w}}{\partial t} + \boldsymbol{w}\cdot\nabla\boldsymbol{w} + 2\omega_0 \boldsymbol{e}_3 \times \boldsymbol{w} + \omega_0^2 \boldsymbol{e}_3 \times (\boldsymbol{e}_3 \times \boldsymbol{x})\right)$$
$$= -\nabla P + \mu \Delta \boldsymbol{w} + \rho\Big(\boldsymbol{g} - \frac{\mathrm{d}\boldsymbol{v}_p}{\mathrm{d}t} - 2\omega_0 \boldsymbol{e}_3 \times \boldsymbol{v}_p - \omega_0^2 \boldsymbol{e}_3 \times (\boldsymbol{e}_3 \times \boldsymbol{x}_p)\Big), \tag{2.2}$$

$$\boldsymbol{w} = \boldsymbol{\omega}_p \times \boldsymbol{x}, \quad |\boldsymbol{x}| = a, \quad \boldsymbol{w} \to -\boldsymbol{v}_p, \quad |\boldsymbol{x}| \to \infty, \tag{2.3}$$

where the particle's rotation $\boldsymbol{\omega}_p$, position $\boldsymbol{x}_p$ and velocity $\boldsymbol{v}_p$ are relative to the co-rotating reference frame of the bulk fluid (i.e. where the unperturbed velocity field is null). By introducing the classical decomposition $(\boldsymbol{w}^0, P^0) + (\boldsymbol{w}^1, P^1)$ (unperturbed and perturbation fields), and since in the present reference frame $\boldsymbol{w}^0 = -\boldsymbol{v}_p$ we can check that the non-dimensional equations for $\boldsymbol{w}^1(\boldsymbol{x}, t)$ are

$$\nabla \cdot \boldsymbol{w}^1 = 0, \tag{2.4}$$

$$Ta\frac{\partial \boldsymbol{w}^1}{\partial t} + Ta 2\boldsymbol{e}_3 \times \boldsymbol{w}^1 + Re(-\boldsymbol{v}_p \cdot \nabla \boldsymbol{w}^1 + \boldsymbol{w}^1 \cdot \nabla \boldsymbol{w}^1) = -\nabla P^1 + \Delta \boldsymbol{w}^1, \tag{2.5}$$

$$\boldsymbol{w}^1 = \boldsymbol{v}_p + \boldsymbol{\omega}_p \times \boldsymbol{x}, \qquad |\boldsymbol{x}| = 1, \quad \boldsymbol{w}^1 \to \boldsymbol{0}, \qquad |\boldsymbol{x}| \to \infty. \tag{2.6}$$

(Note that (2.4)–(2.6) have been normalized by using a for length, $|\boldsymbol{v}_p|$ for velocities, $1/\omega_0$ for the time derivative, and $\mu|\boldsymbol{v}_p|/a$ for pressure, but for the sake of simplicity, the notation has not changed.)

Keeping in mind that in the present investigation, both the Taylor and the Reynolds numbers are assumed to be small compared to unity, we can see (if the order of the unsteady term is not too large) that the near field of $\boldsymbol{w}^1$ should be dominated by a steady creeping flow. Following the classical approach, we can therefore point out, by using the analytical expression of a Stokes flow, that the Coriolis term (second term of the left-hand side of (2.5)), balances the viscous term at a distance from the particle given by $a/Ta^{1/2}$ (the Ekman length), whereas the convective terms balance the viscous term at a distance given by a/Re (the Oseen length). Under the premise $Ta^{1/2} \gg Re$, Coriolis inertia effects therefore dominate convective inertia effects.

Let us now discuss the flow induced by the particle's rotation. In the creeping-flow limit the angular velocity of the particle is expected to match closely that of the bulk fluid, since no external torques act on the particle (see for instance Childress 1964). In the present analysis, the deviation of the particle's rotation from the angular

velocity of the bulk fluid is expected to scale with some power of Ta (or Re), and can therefore only contributes to the force acting on the particle at a level smaller than that being evaluated here.

Note that in this type of investigation concerning small-Reynolds-number flows, it is generally assumed that the particle's rotation plays no role in the determination of the leading order of the induced force. (For instance, in the famous problem addressed by Saffman 1965, the particle obviously experiences a hydrodynamic torque, but the particle's rotation is not taken into account when the lift force is carried out.)

Finally, if (2.5) and (2.6) are re-written, by keeping only the terms that are expected to play a role in the calculation of the induced force, we are led to

$$Ta\left(\frac{\partial \boldsymbol{w}^1}{\partial t} + 2\boldsymbol{e}_3 \times \boldsymbol{w}^1\right) = -\nabla P^1 + \Delta \boldsymbol{w}^1, \tag{2.7}$$

$$\boldsymbol{w}^1 \to 0, \qquad |\boldsymbol{x}| \to \infty, \quad \boldsymbol{w}^1 = \boldsymbol{v}_p(t), \qquad |\boldsymbol{x}| = 1. \tag{2.8}$$

We now introduce the temporal inverse Fourier transform

$$\mathscr{F}_t^{-1}\left(\boldsymbol{v}_p^{\Omega}\right) = \frac{1}{2\pi}\int_{\mathbb{R}} \boldsymbol{v}_p^{\Omega} \exp(-\mathrm{i}\Omega t)\,\mathrm{d}\Omega = \boldsymbol{v}_p(t), \tag{2.9}$$

keeping in mind that $\Omega = \omega/\omega_0$. If $\boldsymbol{F}^{\Omega}\exp(-\mathrm{i}\Omega t)$ is the force acting on a particle which is moving with the following velocity

$$\boldsymbol{v}_p(t) = \boldsymbol{v}_p^{\Omega}\exp(-\mathrm{i}\Omega t), \tag{2.10}$$

then the force acting on a particle moving arbitrarily is given by

$$\boldsymbol{F}^1(t) = \frac{1}{2\pi}\int_{\mathbb{R}} \boldsymbol{F}^{\Omega}\exp(-\mathrm{i}\Omega t)\,\mathrm{d}\Omega, \tag{2.11}$$

since the problem under study is linear. Deriving the force acting on a particle which is oscillating is therefore of fundamental interest in the present investigation. In what follows, this force (i.e. $\boldsymbol{F}^{\Omega}$) will be obtained by means of matched asymptotic expansions. Rigorously speaking, this method can be applied only if the solution of (2.7) corresponds, near the particle and at leading order, to a steady creeping flow, since the particle will be replaced by a point force, the strength of which corresponds to a steady Stokes drag. According to (2.10), the order of the unsteady term involved in (2.7) is given by $Ta\Omega$, so that this term is required to be small and we first assume that this condition is fulfilled. However, for later convenience, let us specify that since we also have $Ta \ll 1$, Ω can nevertheless be much greater than unity.

In the present investigation, it turns out that the induced force acting on a particle moving along the fluid rotation axis is totally decoupled from the force acting on a particle which is moving perpendicularly. This property is useful since it allows us to consider each case separately. Accordingly, let us first deal with the condition:

$$\boldsymbol{v}_p = w_p^{\Omega}\exp(-\mathrm{i}\Omega t)\boldsymbol{e}_3. \tag{2.12}$$

As said before, and following the classical approach, it is assumed that in the vicinity of the particle (inner problem), the induced flow corresponds to a steady Stokes flow plus a corrective term that scales as $Ta^{1/2}$. This inner flow must match the solution of the outer problem:

$$\frac{\partial \boldsymbol{w}^1}{\partial t} + 2\boldsymbol{e}_3 \times \boldsymbol{w}^1 = -\nabla P^1 + \Delta \boldsymbol{w}^1 + 6\pi w_p^{\Omega}\exp(-\mathrm{i}\Omega t)\delta(\boldsymbol{x})\boldsymbol{e}_3, \tag{2.13}$$

where the particle is replaced by the classical Dirac source term. (Note that in the classical matched asymptotic expansions method, this equation is usually written using stretched coordinates, but for the sake of simplicity, we have not changed the notations.) Equation (2.13) is usually solved by making use of the spatial Fourier transform defined as

$$\tilde{\boldsymbol{w}}(\boldsymbol{k},t)=\frac{1}{8\pi^3}\int_{\mathbb{R}^3}\boldsymbol{w}^1(\boldsymbol{x},t)\exp(-\mathrm{i}\boldsymbol{k}\cdot\boldsymbol{x})\,\mathrm{d}^3\boldsymbol{x}, \tag{2.14}$$

and we are led to

$$\frac{\partial\tilde{\boldsymbol{w}}}{\partial t}+2\boldsymbol{e}_3\times\tilde{\boldsymbol{w}}=-\mathrm{i}\boldsymbol{k}\tilde{P}-k^2\tilde{\boldsymbol{w}}+\frac{3w_p^{\Omega}}{4\pi^2}\exp(-\mathrm{i}\Omega t)\boldsymbol{e}_3. \tag{2.15}$$

Because the solution is periodic, and because it also depends linearly on the value of w_p^{Ω}, it is convenient to seek the solution of (2.15) in the form

$$\tilde{\boldsymbol{w}}=\tilde{\boldsymbol{w}}^{\Omega}w_p^{\Omega}\exp(-\mathrm{i}\Omega t),\quad \tilde{P}=\tilde{P}^{\Omega}w_p^{\Omega}\exp(-\mathrm{i}\Omega t), \tag{2.16}$$

which yields

$$-\mathrm{i}\Omega\tilde{\boldsymbol{w}}^{\Omega}+2\boldsymbol{e}_3\times\tilde{\boldsymbol{w}}^{\Omega}=-\mathrm{i}\boldsymbol{k}\tilde{P}^{\Omega}-k^2\tilde{\boldsymbol{w}}^{\Omega}+\frac{3}{4\pi^2}\boldsymbol{e}_3. \tag{2.17}$$

By injecting $\tilde{\boldsymbol{w}}^{\Omega}=\tilde{u}^{\Omega}\boldsymbol{e}_1+\tilde{v}^{\Omega}\boldsymbol{e}_2+\tilde{w}^{\Omega}\boldsymbol{e}_3$ into (2.17), and using the continuity equation (i.e. $\boldsymbol{k}\cdot\tilde{\boldsymbol{w}}^{\Omega}=0$), we obtain an algebraic system with four unknowns ($\tilde{u}^{\Omega}$, $\tilde{v}^{\Omega}$, $\tilde{w}^{\Omega}$, $\tilde{P}^{\Omega}$) which is solved analytically. In this matched asymptotic expansion approach, the non-dimensional force correction that must be added to the Stokes' drag and that we shall note $\boldsymbol{F}^c$, is given (see for instance Saffman 1965) by

$$\boldsymbol{F}^c=6\pi\sqrt{Ta}w_p^{\Omega}\exp(-\mathrm{i}\Omega t)\boldsymbol{e}_3\int_{\mathbb{R}^3}\left(\tilde{w}^{\Omega}-\tilde{w}_s^{\Omega}\right)\mathrm{d}^3\boldsymbol{k}, \tag{2.18}$$

where $\tilde{w}_s^{\Omega}$ corresponds to the solution of (2.17) with the left-hand side set to 0 (Stokes problem). Note that in order to use the same notation as Miyazaki, we also write

$$-h(\Omega)=\int_{\mathbb{R}^3}\left(\tilde{w}^{\Omega}-\tilde{w}_s^{\Omega}\right)\mathrm{d}^3\boldsymbol{k}. \tag{2.19}$$

The calculation of this integral is tedious, and intermediary results are not very interesting, so we specify here only how the final result is obtained. First, we introduce cylindrical coordinates in the Fourier space, following for example Gotoh (1990), $k_1=-\hat{k}\sin(\eta)$ and $k_2=\hat{k}\cos(\eta)$:

$$-h(\Omega)=\int_{-\infty}^{\infty}\int_0^{\infty}\int_0^{2\pi}\left(\tilde{w}^{\Omega}-\tilde{w}_s^{\Omega}\right)\hat{k}\,\mathrm{d}\eta\,\mathrm{d}\hat{k}\,\mathrm{d}k_3, \tag{2.20}$$

and we perform the intermediate integration:

$$I(\Omega)=\int_0^{2\pi}\left(\tilde{w}^{\Omega}-\tilde{w}_s^{\Omega}\right)\mathrm{d}\eta. \tag{2.21}$$

Secondly, we set $k_3=k'\sin(\phi)$ and $\hat{k}=k'\cos(\phi)$. This yields

$$-h(\Omega)=\int_0^{\infty}\int_{-\pi/2}^{\pi/2}I(\Omega)k'^2\cos(\phi)\,\mathrm{d}\phi\,\mathrm{d}k', \tag{2.22}$$

and this last integral can be calculated analytically. We are led to

$$h(\Omega) = \frac{\mathrm{i}}{70}\Bigg(- \frac{\Omega^4}{\sqrt{-\mathrm{i}(\Omega-2)}} + \frac{\Omega^4}{\sqrt{-\mathrm{i}(\Omega+2)}} + \frac{\Omega^3}{\sqrt{-\mathrm{i}(\Omega-2)}} + \frac{\Omega^3}{\sqrt{-\mathrm{i}(\Omega+2)}} + \frac{18\Omega^2}{\sqrt{-\mathrm{i}(\Omega-2)}} - \frac{18\Omega^2}{\sqrt{-\mathrm{i}(\Omega+2)}} - \frac{52\Omega}{\sqrt{-\mathrm{i}(\Omega-2)}} - \frac{52\Omega}{\sqrt{-\mathrm{i}(\Omega+2)}} + \frac{40}{\sqrt{-\mathrm{i}(\Omega-2)}} - \frac{40}{\sqrt{-\mathrm{i}(\Omega+2)}}\Bigg). \tag{2.23}$$

We now consider the case of a particle oscillating along $\boldsymbol{e}_1$ (i.e. perpendicularly to the rotation axis):

$$\boldsymbol{v}_p = u_p^{\Omega} \exp(-\mathrm{i}\Omega t)\boldsymbol{e}_1. \tag{2.24}$$

The outer problem is now

$$\frac{\partial \boldsymbol{w}^1}{\partial t} + 2\boldsymbol{e}_3 \times \boldsymbol{w}^1 = -\nabla P^1 + \Delta \boldsymbol{w}^1 + 6\pi u_p^{\Omega} \exp(-\mathrm{i}\Omega t)\delta(\boldsymbol{x})\boldsymbol{e}_1, \tag{2.25}$$

and following the same approach as that described previously, the force correction acting on the particle is now given by

$$\boldsymbol{F}^c = 6\pi\sqrt{Ta}u_p^{\Omega} \exp(-\mathrm{i}\Omega t)\,(-f(\Omega)\boldsymbol{e}_1 - g(\Omega)\boldsymbol{e}_2)\,, \tag{2.26}$$

where once again we have written

$$-f(\Omega) = \int_{\mathbb{R}^3} (\tilde{u}^{\Omega} - \tilde{u}_s^{\Omega})\,\mathrm{d}^3\boldsymbol{k}, \quad -g(\Omega) = \int_{\mathbb{R}^3} (\tilde{v}^{\Omega} - \tilde{v}_s^{\Omega})\,\mathrm{d}^3\boldsymbol{k}. \tag{2.27}$$

The calculation of these integrals can be performed in the same way as before, and this time we are led to

$$f(\Omega) = -\frac{\mathrm{i}}{140}\Bigg(- \frac{\Omega^4}{\sqrt{-\mathrm{i}(\Omega-2)}} + \frac{\Omega^4}{\sqrt{-\mathrm{i}(\Omega+2)}} + \frac{\Omega^3}{\sqrt{-\mathrm{i}(\Omega-2)}} + \frac{\Omega^3}{\sqrt{-\mathrm{i}(\Omega+2)}} - \frac{17\Omega^2}{\sqrt{-\mathrm{i}(\Omega-2)}} + \frac{17\Omega^2}{\sqrt{-\mathrm{i}(\Omega+2)}} + \frac{88\Omega}{\sqrt{-\mathrm{i}(\Omega-2)}} + \frac{88\Omega}{\sqrt{-\mathrm{i}(\Omega+2)}} - \frac{100}{\sqrt{-\mathrm{i}(\Omega-2)}} + \frac{100}{\sqrt{-\mathrm{i}(\Omega+2)}}\Bigg) \tag{2.28}$$

and

$$g(\Omega) = \frac{\mathrm{i}}{20}\Bigg(\frac{(\Omega-2)}{|\Omega-2|}\frac{\Omega^3}{\sqrt{\mathrm{i}(\Omega-2)}} - \frac{(2+\Omega)}{|2+\Omega|}\frac{\Omega^3}{\sqrt{\mathrm{i}(\Omega+2)}} - \frac{(\Omega-2)}{|\Omega-2|}\frac{\Omega^2}{\sqrt{\mathrm{i}(\Omega-2)}} - \frac{(2+\Omega)}{|2+\Omega|}\frac{\Omega^2}{\sqrt{\mathrm{i}(\Omega+2)}} - \frac{(\Omega-2)}{|\Omega-2|}\frac{8\Omega}{\sqrt{\mathrm{i}(\Omega-2)}} + \frac{(2+\Omega)}{|2+\Omega|}\frac{8\Omega}{\sqrt{\mathrm{i}(\Omega+2)}} + \frac{(\Omega-2)}{|\Omega-2|}\frac{12}{\sqrt{\mathrm{i}(\Omega-2)}} + \frac{(2+\Omega)}{|2+\Omega|}\frac{12}{\sqrt{\mathrm{i}(\Omega+2)}}\Bigg). \tag{2.29}$$

Note that by using the symmetrical properties of the problem, we can check that if the particle were oscillating along $\boldsymbol{e}_2$, instead of $\boldsymbol{e}_1$, the corresponding force would be given by

$$\boldsymbol{F}^c = 6\pi\sqrt{Ta}v_p^{\Omega} \exp(-i\Omega t)\,(g(\Omega)\boldsymbol{e}_1 - f(\Omega)\boldsymbol{e}_2)\,, \tag{2.30}$$

so we need not deal explicitly with that case. If the velocity of the particle is given by (2.10), then the force acting on it can be drawn by superimposing these previous

results and is

$$\boldsymbol{F}^{\Omega} = -6\pi(\boldsymbol{I} + \sqrt{Ta}\boldsymbol{M}(\Omega) + O(Ta))\cdot \boldsymbol{v}_p^{\Omega}, \tag{2.31}$$

where $\boldsymbol{M}(\Omega)$ is the tensor given by (1.7), but where $f(\Omega)$, $g(\Omega)$ and $h(\Omega)$ are now given by (2.23), (2.28) and (2.29). In spite of their complex analytical expressions, we can check that these three functions are continuous, even for $\Omega = \pm 2$. In particular, when $|\Omega| \leqslant 2$, we can check that these functions can be factorized and written under the same form as (1.8), (1.9) and (1.10). (However, this factorized form is no longer valid when $|\Omega| > 2$ and it is likely that Miyazaki obtained the same results as those derived here, but published them only in this factorized form.)

Note that so far, (2.23), (2.28) and (2.29) are valid only in the limit of weak unsteadiness, $Ta\Omega = a^2\omega/\nu \ll 1$, as required by the method used. Fortunately, this problem can be readily overpassed. On one hand, when $a^2\omega/\nu \gg 1$, (2.7) degenerates into the unsteady creeping-flow equation, since the unsteady term dominates the Coriolis term. The corresponding force is therefore given by the well-known Boussinesq–Basset–Oseen (BBO) force which can be written (see for example Landau & Lifchitz 1989):

$$\boldsymbol{F}^{\Omega} = -6\pi\mu a\left(1 + \sqrt{Ta}\frac{\sqrt{2}}{2}(1-\mathrm{i})\sqrt{\Omega} + \frac{Ta}{9}(-\mathrm{i}\Omega)\right)\boldsymbol{v}_p^{\Omega}. \tag{2.32}$$

On the other hand, when $\Omega \gg 1$, we can check that

$$\lim_{\Omega\gg 1} f(\Omega) = \lim_{\Omega\gg 1} h(\Omega) = \frac{\sqrt{2}}{2}(1-\mathrm{i})\sqrt{\Omega} + O\left(\Omega^{-3/2}\right), \quad \lim_{\Omega\gg 1} g(\Omega) = O\left(\Omega^{-1/2}\right), \tag{2.33}$$

so that the $O(Ta^{1/2})$ terms of (2.31) match those of (2.32). This allows us to conclude that (2.31) is valid, whatever the value of Ω, without any restrictions. (This point is required to perform the calculations in the following section.)

3. Force $\boldsymbol{F}^1$ for the arbitrary motion of a particle

We now derive the force in the time domain, performing the calculation of $\mathscr{F}_t^{-1}(\boldsymbol{F}^{\Omega})$ given by (2.11). To achieve this calculation, we first establish the following intermediary results (see Appendix):

$$\mathscr{F}_t^{-1}\left(\frac{1}{\sqrt{-\mathrm{i}(\Omega+2)}}\right) = \frac{\exp(2\mathrm{i}t)}{\sqrt{\pi t}}, \quad \mathscr{F}_t^{-1}\left(\frac{1}{\sqrt{-\mathrm{i}(\Omega-2)}}\right) = \frac{\exp(-2\mathrm{i}t)}{\sqrt{\pi t}}, \tag{3.1a, b}$$

$$\mathscr{F}_t^{-1}\left(\frac{(2+\Omega)/|2+\Omega|}{\sqrt{\mathrm{i}(\Omega+2)}}\right) = -\frac{\mathrm{i}\exp(2\mathrm{i}t)}{\sqrt{\pi t}}, \quad \mathscr{F}_t^{-1}\left(\frac{(\Omega-2)/|\Omega-2|}{\sqrt{\mathrm{i}(\Omega-2)}}\right) = -\frac{\mathrm{i}\exp(-2\mathrm{i}t)}{\sqrt{\pi t}}. \tag{3.2a, b}$$

Secondly, we also use the following properties

$$\mathscr{F}_t^{-1}\left((-\mathrm{i}\Omega)^m a(\Omega)\boldsymbol{v}_p^{\Omega}\right) = \frac{\mathrm{d}^{m-1}\mathscr{F}_t^{-1}(a(\Omega))}{\mathrm{d}t^{m-1}} * \frac{\mathrm{d}\boldsymbol{v}_p(t)}{\mathrm{d}t} \tag{3.3}$$

and

$$\mathscr{F}_t^{-1}\left(a(\Omega)\boldsymbol{v}_p^{\Omega}\right) = \mathscr{F}_t^{-1}(a(\Omega)) * \boldsymbol{v}_p(t), \tag{3.4}$$

which are valid for any non-zero integer m, and for any functions involved in (3.1) or (3.2) (written $a(\Omega)$, for the sake of simplicity). Note that the symbol * stands for

the temporal convolution product. According to the results obtained in the previous section, the force acting on a particle moving arbitrarily is

$$\boldsymbol{F}^1(t) = -6\pi\left(\boldsymbol{v}_p(t) + \sqrt{Ta}\left(\int_0^t \boldsymbol{K}_1(t-\tau)\cdot\frac{\mathrm{d}\boldsymbol{v}_p(\tau)}{\mathrm{d}\tau}\,\mathrm{d}\tau + \int_0^t \boldsymbol{K}_2(t-\tau)\cdot\boldsymbol{v}_p(\tau)\,\mathrm{d}\tau\right) + O(Ta)\right), \tag{3.5}$$

where $\boldsymbol{K}_1(t)$ is a tensor

$$\boldsymbol{K}_1(t) = \begin{pmatrix} f_1(t) & -g_1(t) & 0 \\ g_1(t) & f_1(t) & 0 \\ 0 & 0 & h_1(t) \end{pmatrix} \tag{3.6}$$

and

$$f_1(t) = \frac{1}{112}\left(\frac{80\cos(2t)t^3 + 20\sin(2t)t^2 + 6\cos(2t)t - 3\sin(2t))}{t^3\sqrt{\pi t}}\right), \tag{3.7}$$

$$g_1(t) = -\frac{3}{40}\left(\frac{8\sin(2t)t^2 - 2\cos(2t)t + \sin(2t)}{t^2\sqrt{\pi t}}\right), \tag{3.8}$$

$$h_1(t) = \frac{1}{56}\left(\frac{32\cos(2t)t^3 + 8\sin(2t)t^2 - 6\cos(2t)t + 3\sin(2t))}{t^3\sqrt{\pi t}}\right), \tag{3.9}$$

and where

$$\boldsymbol{K}_2(t) = \begin{pmatrix} f_2(t) & -g_2(t) & 0 \\ g_2(t) & f_2(t) & 0 \\ 0 & 0 & h_2(t) \end{pmatrix}, \tag{3.10}$$

$$f_2(t) = \frac{10}{7}\frac{\sin(2t)}{\sqrt{\pi t}}, \quad g_2(t) = \frac{6}{5}\frac{\cos(2t)}{\sqrt{\pi t}}, \quad h_2(t) = \frac{8}{7}\frac{\sin(2t)}{\sqrt{\pi t}}. \tag{3.11}$$

In order to ensure the validity of (3.5), we now test it by recovering some of the results presented in § 1. We first analyse the behaviour of the force corresponding to a sudden motion of the particle, that is $\mathrm{d}\boldsymbol{v}_p(t)/\mathrm{d}t = \delta(t)$ or equivalently $\boldsymbol{v}_p(t) = H(t)$ ($H(t)$ is the Heaviside function) where (3.5) is expected to tend towards the results of Herron *et al.* (1975). Figure 1(*a*) shows the response of the induced force in such a case. At short times ($t \ll 1$), we recognize the behaviour of the classical BBO force since

$$f_1(t) \sim h_1(t) \sim \frac{1}{\sqrt{\pi t}}, \quad g_1(t) \sim -\frac{7}{5}\frac{\sqrt{t}}{\sqrt{\pi}}, \tag{3.12}$$

$$\int_0^t f_2(t)\,\mathrm{d}t \sim \frac{40}{21}\frac{t^{3/2}}{\sqrt{\pi}}, \quad \int_0^t g_2(t)\,\mathrm{d}t \sim \frac{12}{5}\frac{\sqrt{t}}{\sqrt{\pi}}, \quad \int_0^t h_2(t)\,\mathrm{d}t \sim \frac{32}{21}\frac{t^{3/2}}{\sqrt{\pi}}. \tag{3.13}$$

Figure 1(*b*) is an enlargement of figure 1(*a*) around the asymptotical values reached by three functions plotted in figure 1(*a*). At long times, Herron's results are well retrieved, and we obtain

$$f_1(t) \sim g_1(t) \sim h_1(t) \sim O(1/\sqrt{t}), \tag{3.14}$$

$$\int_0^t f_2(t)\,\mathrm{d}t \sim \tfrac{5}{7}, \quad \int_0^t g_2(t)\,\mathrm{d}t \sim \tfrac{3}{5}, \quad \int_0^t h_2(t)\,\mathrm{d}t \sim \tfrac{4}{7}. \tag{3.15}$$

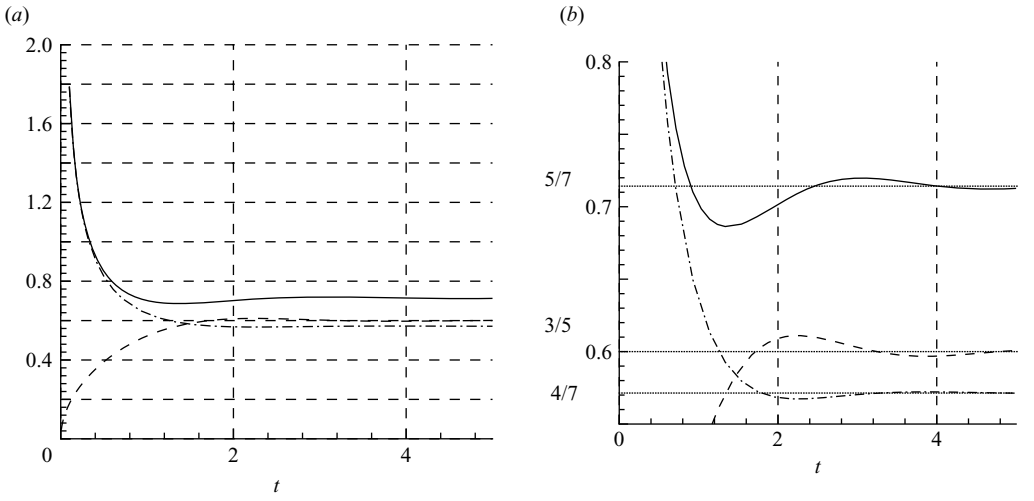

FIGURE 1. (*a*) Temporal evolution of the force correction in response to a sudden start motion. (*b*) Enlargement of the same three functions around their asymptotic (steady) values. —, $f_1(t) + \int_0^t f_2(\tau)\,\mathrm{d}\tau$; ---, $g_1(t) + \int_0^t g_2(\tau)\,\mathrm{d}\tau$; – · –, $h_1(t) + \int_0^t h_2(\tau)\,\mathrm{d}\tau$.

We can also observe that the typical (dimensional) time taken by the force to reach its steady value scales as $1/\omega_0$. This is physically sound, since this time scale corresponds to the time taken by the vorticity (created by the change of velocity), to diffuse to the distance $a/\sqrt{Ta}$, were the Coriolis term, involved in the induced-flow equations, balances the viscous term.

Figure 1(*b*) also shows that the force reaches its steady value after a decayed oscillating regime. (Note that similar behaviour had already been observed by Wakaba & Balachandar 2005, who performed numerical simulation involving a particle immersed in a shear flow and at moderate Reynolds numbers).

Another situation that can be used corresponds to the case of a particle kept fixed in the laboratory reference frame. Its velocity is therefore given by $\boldsymbol{v}_p = \cos(t)\boldsymbol{e}_1 - \sin(t)\boldsymbol{e}_2$ in the co-rotating reference frame and the horizontal components of the tensor $\boldsymbol{M}$ can be carried out by using simply the results (2.28) and (2.29), since we can write

$$\boldsymbol{M}\cdot\boldsymbol{v}_p = \mathrm{Re}[\boldsymbol{M}(\Omega = 1)\cdot \exp(-\mathrm{i}t)\boldsymbol{e}_1] + \mathrm{Im}[\boldsymbol{M}(\Omega = 1)\cdot \exp(-\mathrm{i}t)\boldsymbol{e}_2], \tag{3.16}$$

where Re( ) and Im( ) denote the real and imaginary parts, respectively. Gotoh's results, given in (1.6), are recovered as expected.

4. Force acting on a particle in the laboratory reference frame

In the previous section, we derived the induced force acting on a particle in the co-rotating reference frame, and this force should be inserted into (1.3) in order to predict the particle's dynamics. However, it may be useful, sometimes, to deal with a motion equation written in the laboratory reference frame instead of in the co-rotating reference frame. In what follows, we derive the expression of the induced force (3.5) in the laboratory (absolute) reference frame. Note that this transformation must be done cautiously since (3.5) involves convolution products, and therefore both the history of the time dependence of the particle velocity and of the particle acceleration in the co-rotating frame must be taken into account explicitly during the translation to the laboratory reference frame, as pointed out by Miyazaki (1995). Following his

approach, if $\boldsymbol{x}_p$ denotes the particle position in the co-rotating reference frame, and $\boldsymbol{x}_p^a$ denotes the particle position in the absolute reference frame (in the following, the superscript a indicates that the vector is written in the laboratory (absolute) reference frame), we have the relations

$$\boldsymbol{x}_p^a(t) = \boldsymbol{P}(t)\cdot\boldsymbol{x}_p(t) \quad \text{where} \quad \boldsymbol{P} = \begin{pmatrix} \cos t & -\sin t & 0 \\ \sin t & \cos t & 0 \\ 0 & 0 & 1 \end{pmatrix}, \tag{4.1}$$

if the vector is written in the laboratory reference frame, or

$$\boldsymbol{x}_p(t) = \boldsymbol{P}^t(t)\cdot\boldsymbol{x}_p^a(t), \tag{4.2}$$

if the vector is written in the co-rotating reference frame. (Note that the superscript t stands for the transposition.) Let us now introduce the following tensor

$$\boldsymbol{\Omega} = \begin{pmatrix} 0 & -1 & 0 \\ 1 & 0 & 0 \\ 0 & 0 & 0 \end{pmatrix}, \tag{4.3}$$

which satisfies the relation: $\boldsymbol{\Omega}\cdot\boldsymbol{x}_p = \boldsymbol{e}_3 \times \boldsymbol{x}_p$. We can readily check that

$$\frac{\mathrm{d}\boldsymbol{P}^t}{\mathrm{d}t} = -\boldsymbol{\Omega}\cdot\boldsymbol{P}^t, \tag{4.4}$$

and using this result allows us to write

$$\frac{\mathrm{d}\boldsymbol{x}_p}{\mathrm{d}t} = \boldsymbol{v}_p = \boldsymbol{P}^t\cdot\left(\frac{\mathrm{d}\boldsymbol{x}_p^a}{\mathrm{d}t} - \boldsymbol{\Omega}\cdot\boldsymbol{x}_p^a\right) = \boldsymbol{P}^t\cdot\boldsymbol{v}_s^a \tag{4.5}$$

where $\boldsymbol{v}_s^a$ is the particle's slip velocity, relative to the laboratory reference frame. (Note that $\boldsymbol{P}^t$ and $\boldsymbol{\Omega}$ are both antisymmetric so that they can commute.) Similarly, we obtain, for the particle acceleration:

$$\frac{\mathrm{d}\boldsymbol{v}_p}{\mathrm{d}t} = \boldsymbol{P}^t\left(\frac{\mathrm{d}\boldsymbol{v}_s^a}{\mathrm{d}t} - \boldsymbol{\Omega}\cdot\boldsymbol{v}_s^a\right), \tag{4.6}$$

and the two integrals in (3.5) can be re-written as follows:

$$\int_0^t \boldsymbol{K}_1(t-\tau)\cdot\frac{\mathrm{d}\boldsymbol{v}_p(\tau)}{\mathrm{d}\tau}\,\mathrm{d}\tau = \int_0^t \boldsymbol{K}_1(t-\tau)\cdot\left(\boldsymbol{P}^t(\tau)\cdot\frac{\mathrm{d}\boldsymbol{v}_s^a(\tau)}{\mathrm{d}\tau} - \boldsymbol{P}^t(\tau)\cdot\boldsymbol{\Omega}\cdot\boldsymbol{v}_s^a(\tau)\right)\mathrm{d}\tau, \tag{4.7}$$

$$\int_0^t \boldsymbol{K}_2(t-\tau)\cdot\boldsymbol{v}_p(\tau)\,\mathrm{d}\tau = \int_0^t \boldsymbol{K}_2(t-\tau)\cdot\left(\boldsymbol{P}^t(\tau)\cdot\boldsymbol{v}_s^a(\tau)\right)\mathrm{d}\tau. \tag{4.8}$$

Note that so far, these terms are written in the co-rotating reference frame, even if they involves the particle slip velocity and the particle acceleration written in the laboratory reference frame. However, the transformation back to the laboratory reference frame is now straightforward since

$$\boldsymbol{F}^{1a} = \boldsymbol{P}(t)\cdot\boldsymbol{F}^1. \tag{4.9}$$

By using again the commutativity of the tensors, and since

$$\boldsymbol{P}(t)\cdot\boldsymbol{P}^t(\tau) = \boldsymbol{P}(t-\tau), \tag{4.10}$$

we are led to

$$\boldsymbol{F}^{1a} = -6\pi\left(\boldsymbol{v}_s^a(t) + \sqrt{Ta}\left(\int_0^t \boldsymbol{K}_1^a(t-\tau)\cdot\frac{\mathrm{d}\boldsymbol{v}_s^a}{\mathrm{d}t}\,\mathrm{d}\tau + \int_0^t \boldsymbol{K}_2^a(t-\tau)\cdot\boldsymbol{v}_s^a(\tau)\,\mathrm{d}\tau\right)\right) \tag{4.11}$$

where

$$\boldsymbol{K}_1^a = \boldsymbol{K}_1 \cdot \boldsymbol{P}, \quad \boldsymbol{K}_2^a = (\boldsymbol{K}_2 - \boldsymbol{K}_1 \cdot \boldsymbol{\Omega}) \cdot \boldsymbol{P}. \tag{4.12}$$

In the laboratory reference frame, the particle motion equation is therefore given by

$$m_p \frac{\mathrm{d}\boldsymbol{v}_p^a}{\mathrm{d}t} = (m_p - m_f)\boldsymbol{g}^a + m_f \omega_0^2 \boldsymbol{e}_3 \times \left(\boldsymbol{e}_3 \times \boldsymbol{x}_p^a\right) + \boldsymbol{F}^{1a}(t), \tag{4.13}$$

where the second term of the right-hand side now corresponds to the classical pressure gradient of the unperturbed flow (i.e. $m_f \mathrm{D}\boldsymbol{v}^a/\mathrm{D}t$), in the particular case of a solid-body rotating fluid. In what follows, (4.13) will be illustrated in practical situations.

5. Applications

In this section, we deal with two physical situations where both unsteady and inertia effects modify the force acting on the particle so that the motion equation (4.13) (together with (4.11)) must be used in order to predict the particle dynamics correctly. In addition, we compare results obtained by solving (numerically) this last-mentioned equation (4.13) to those obtained by using two other theories that could have been used in the present state of our knowledge, even if these other theories are incorrect in the situations addressed, since the comparison is interesting. These other theories involve, respectively, the Basset–Boussinesq–Oseen (BBO) force

$$\boldsymbol{F}^{1a} = -\frac{m_f}{2}\frac{\mathrm{d}\boldsymbol{v}_s^a}{\mathrm{d}t} - 6\pi\mu a \left(\boldsymbol{v}_s^a + \left(\frac{a^2}{\nu}\right)^{1/2} \int_0^t \frac{1}{\sqrt{\pi(t-\tau)}} \frac{\mathrm{d}\boldsymbol{v}_s^a(\tau)}{\mathrm{d}\tau}\,\mathrm{d}\tau \right) \tag{5.1}$$

and the Herron's force (translated here to the laboratory reference frame):

$$\boldsymbol{F}^{1a} = -6\pi\mu a \left(1 + Ta^{1/2}\boldsymbol{M}\right)\boldsymbol{v}_s^a, \tag{5.2}$$

where $\boldsymbol{M}$ is given by (1.5). Note that the BBO force is obtained by neglecting all inertia effects, if the induced fluid motion equations are written in a fixed reference frame linked to the particle, whereas the second one is obtained by neglecting all unsteady effects, if the induced-flow equations are written in a co-rotating reference frame.

5.1. *The unsteady problem of Childress*

We now focus our attention on the time taken by a particle to reach its steady terminal velocity, in the problem initially addressed by Childress (1964). We therefore consider the case of a light particle released along the axis of rotation which is, in this example, co-aligned with gravity (i.e. $\boldsymbol{g}^a = -\mathrm{g}^a\boldsymbol{e}_3$). It is assumed that the particle is released at $t = 0$ and $z_p^a = 0$ (z_p^a is the vertical coordinates of the particle), with no initial velocity. The physical parameters chosen are $a = 1.5\,\mathrm{mm}$, $\omega_0 = 15$ rad s^{-1}, $m_p/m_f = 0.1$, $\nu = 2 \times 10^{-4}\,\mathrm{m}^2\,\mathrm{s}^{-1}$. This corresponds to $Ta^{1/2} \simeq 0.4$ and $Re = 0.12$ (Reynolds number is based on the terminal velocity).

The motion equations involving forces (5.1) and (5.2) can be readily solved analytically (for instance, by making use of the Laplace transform for the BBO equation, as is done in Candelier, Angilella and Souhar 2004), but the corresponding analytical solutions are not given explicitly in the present paper since they are not original or very interesting. Figure 2 shows the corresponding velocities, together with the velocity obtained by solving (numerically) the motion equation involving the force (4.11). (The numerical solution has been obtained by using a third-order Adams–Bashforth numerical scheme, and the methodology used in order to deal with

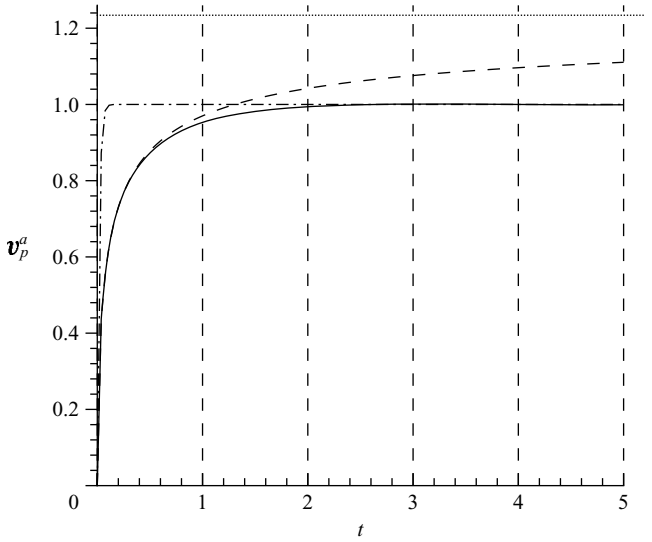

FIGURE 2. Particle velocity normalized by the theoretical terminal velocity predicted by Childress (1964). (Parameters: $a = 1.5\,\text{mm}$, $\omega_0 = 15$ rad s^{-1}, $m_p/m_f = 0.1$, $\nu = 2.10^{-4}$ m^2 s^{-1}. This corresponds to $Ta^{1/2} \simeq 0.4$ and $Re = 0.12$). – – –, force (5.1) (BBO); – · –, force (5.2) (Childress), ——, force (4.11).

the integral term has been previously validated by solving the motion equation with BBO force, where the analytical solution is available.)

At short time, the particle's velocity predicted by using BBO force or by using (4.11) are almost indistinguishable, since at the beginning of the motion, the vorticity generated by the particle's velocity has not yet reached the distance where Coriolis effects start to modify the unsteady creeping flow. In contrast, we can see that the velocity predicted by using the steady force (5.2) is strongly incorrect, since in this case, the particle reaches its terminal velocity almost instantaneously. (Obviously, at short time, the unsteadiness of the induced fluid motion cannot be neglected.)

After a (dimensional) time of the order of $1/\omega_0$, the velocity predicted by the force (4.11) starts to differ from that predicted by using the BBO equation. It therefore tends to the terminal velocity predicted by Childress, whereas the other one tends to the theoretical terminal velocity obtained in the creeping-flow limit and which is strongly overestimated, since no inertia effects are taken into account. Note that inertia effects are not only responsible for a drag increase, but also for a faster relaxation of the kernels of the Basset-like force, in comparison with the classical kernel of BBO force. Therefore, we can check that the particle velocity cannot be predicted by using an empirical motion equation where a steady drag predicted by Childress is added to a BBO force.

5.2. *The motion of a light particle in a horizontal rotating fluid*

In this section, we analyse the motion of a light particle in a horizontal rotating flow. Gravity is now taken perpendicular to the rotation axis (we have set arbitrarily $\boldsymbol{g}^a = -g^a \boldsymbol{e}_2$) and the physical parameters used are the same as in the previous section. We consider, at $t = 0$, that the slip velocity of the particle is null ($\boldsymbol{v}_s^a = \boldsymbol{0}$) and therefore, the particle trajectory takes place in a plane perpendicular to the rotation axis.

The motion equations involving the forces (5.1) or (5.2) can still be solved analytically, even if the resolution is somewhat more complex when compared to

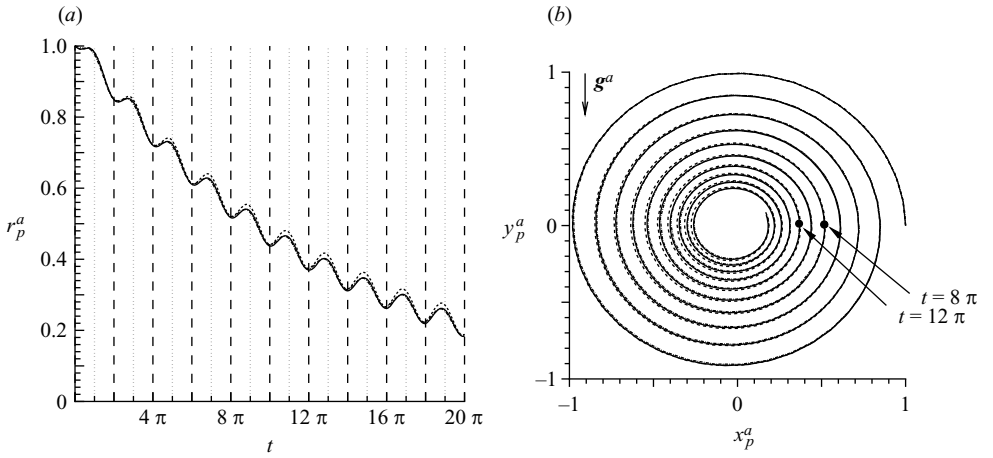

FIGURE 3. (*a*) Temporal evolution of the particle's radial coordinates (distance to the rotation axis) corresponding to various theories for the induced force expression. (*b*) Corresponding trajectories within the plane. Physical parameters used are the same as those of figure 2. The particle's coordinates are normalized by the initial distance to the rotation axis, which has been set arbitrarily to 0.04 cm (dimension of the experimental apparatus of Candelier *et al.* 2005). ——, force (4.11); · · ·, force (5.1) (BBO); – · – force (5.2) (Herron).

the previous (vertical) analysis. We can check that the analytical solution, obtained by using Laplace transform, detailed in Candelier *et al.* (2004) (see also Candelier *et al.* 2005) can be generalized to the case where the gravity is taken into account in the particle's motion equations. (Once again, analytical solutions corresponding to the motion equations involving the forces (5.1) or (5.2) will not be given explicitly here.)

Figure 3(*a*) shows the evolution of the radial coordinates of the particle (i.e. its distance to the rotation axis), and figure 3(*b*) shows the corresponding trajectories observed in the laboratory reference frame, obtained by using the three theories mentioned previously. We observe, at least far from the equilibrium position, that the three theories lead to very close trajectories. Note that a similar phenomenon has been observed by Candelier *et al.* (2005), but for the motion of the particle in a vertical rotating fluid. However, in Candelier & Angilella (2006), it has been pointed out that this similarity was due more to a coincidence than to a physical reason. In contrast, in the present situation, it seems that the similarity may be explained by physical arguments and in particular, by the periodicity of the problem addressed here.

In order to analyse this point, we should mention that according to the particle's location in the plane, the buoyancy force alternatively acts in the same direction as the drag exerted by the fluid on the particle, and in the opposite direction. As a consequence, the particle experiences alternatively accelerations and decelerations. Figure 4 illustrates this phenomena by showing, respectively, the temporal evolutions of the distance to the rotation axis (figure 4*a*), the radial velocity of the particle (figure 4*b*), and the angular rate coordinate (figure 4*c*) (i.e. $\dot{\theta}_p^a$), for t lying between 8π and 12π (figure 3(*b*) shows the respective particle locations at $t = 8\pi$ and at $t = 12\pi$). We can check that during an acceleration phase, discrepancies between the three theories do occur, but they are almost totally compensated by what happens during the following deceleration phase. Therefore, differences between these trajectories do

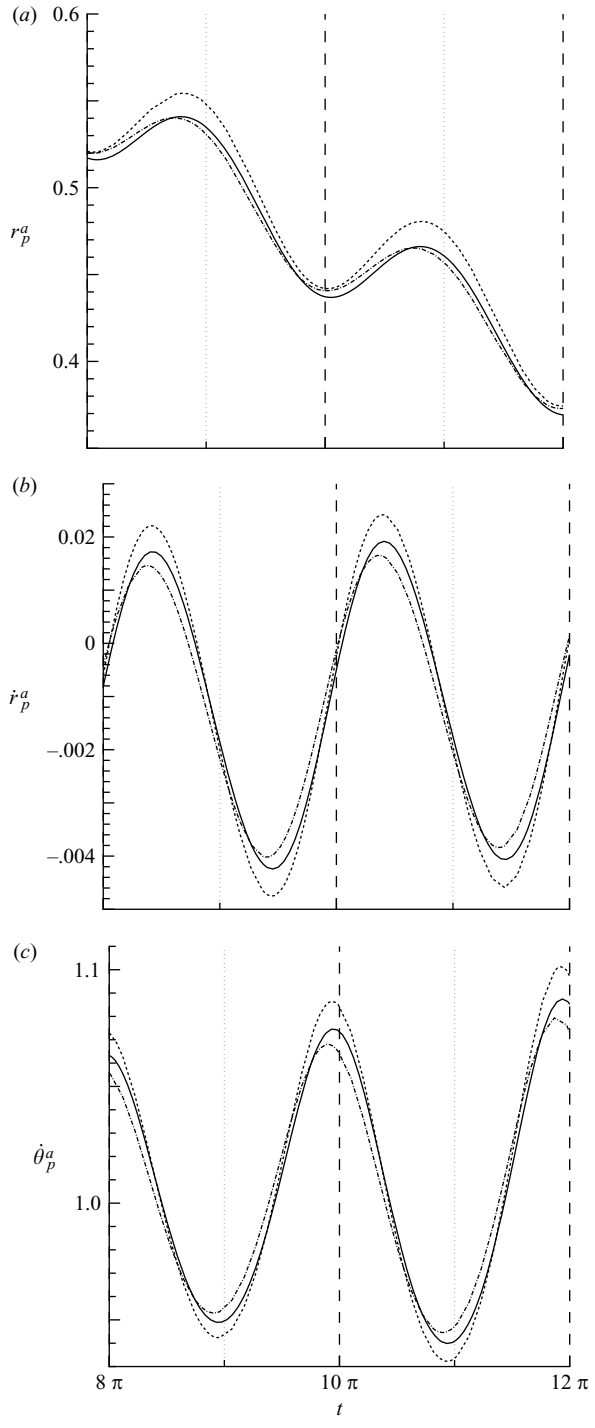

FIGURE 4. (*a*) Enlargement of the temporal evolution of the radial coordinates plotted in figure 3(*a*). (*b*) Temporal evolution of the radial velocity of the particle. (*c*) Temporal evolution of the rotation rate of the particle. Same physical parameters as those of figure 2. ——, force (4.11); · · ·, force (5.1) (BBO); – · –, force (5.2) (Herron).

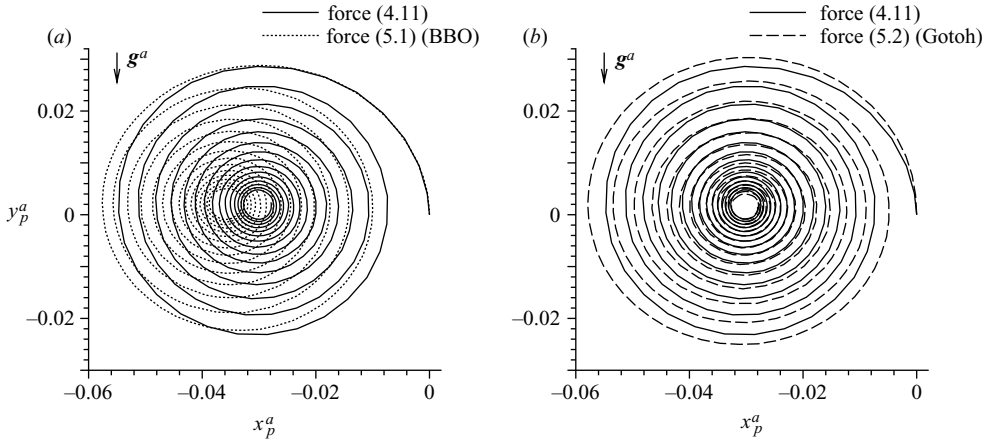

FIGURE 5. Trajectories of the particle in the vicinity of its equilibrium position, involving the force given by (4.11) together with that involving (*a*) the BBO force and (*b*) the Gotoh force. The physical parameters are the same as for figure 2. (The terminal Reynolds number obtained when the particle has reached its equilibrium position is $Re = 0.11$.)

not increase since no accumulation occurs. Note that in each case, the time-averaged (over one turn) of the angular rate is almost equal to unity regardless of the theories used (it is slightly greater than unity), and the time-averaged values for the particle distance and for the radial velocity of the particle are also very close.

A scrupulous analysis of these figures also shows that while the particle is far from its equilibrium position, the trajectory predicted by using Herron's results is closer to that predicted by the force (4.11) than is the trajectory predicted by the BBO force. Actually, this may be explained by using, *a posteriori* the results concerning the particle velocity in these simulations, and we can check that the Coriolis terms of (2.5) dominate the unsteady term (in a rotating reference frame).

That is no longer true when the particle has almost reached its equilibrium position (Note that the theoretical equilibrium position can be drawn by using Gotoh's result). In order to illustrate the dynamics of the particle in the vicinity of this location, we now compare trajectories obtained by using again the force (4.11), BBO force and the force given by (5.2), but where the coefficients of $\boldsymbol{M}$ have now been replaced by Gotoh's results. Figure 5 shows these trajectories, which are quite different for each case. Clearly, the equilibrium position obtained by using the BBO force is not correct since this position is modified by inertia effects.

6. Conclusion

To conclude the present investigation, let us discuss the form of the generalized force (3.5) or equivalently (4.11). Apart from the Stokes drag, this force is composed of two convolution products, one involving the particle acceleration, and the other involving the particle slip velocity.

The term involving the particle acceleration seems quite natural in such an unsteady problem since the force acting on the particle is linked to the vorticity generated by the change of velocity, and therefore, by the particle acceleration. Also, we recover the fact that at short times, this kernel behaves like the BBO kernel (i.e. $1/\sqrt{t}$), since the main process for the vorticity diffusion is due to viscosity, and differs at long times, when inertia effects start to manifest themselves. Note that we are very

familiar with this notion in uniform flow where the BBO kernel is often replaced by another semi-empirical kernel in order to account for inertia effects.

In contrast, we have not discussed the other convolution product involving the particle slip velocity. To explain this term, it may be useful to keep in mind that in a steady problem of a particle immersed in a non-uniform flow, inertia effects on the drag acting on the particle depend only on the slip velocity of the particle. Clearly, inertia-induced forces cannot be generalized to an unsteady case with a term involving the particle acceleration, otherwise it would vanish if the particle reached a steady velocity. In the particular case of the present investigation, we can check that when the unsteadiness of the particle's velocity vanishes, the steady components of the inertia-induced force indeed come from this second integral term. Note that in a paper concerning the unsteady lift force acting on a particle in a linear shear flow (see Candelier & Souhar 2007) it has been also assumed that the result of Asmolov & McLaughlin (1999) could be written under an empirical convolution product involving the slip velocity of the particle.

By playing with words, it may be said that the first integral (involving the particle acceleration) can be seen as an unsteady force perturbed by an inertia effect, whereas the second one is an inertia-induced force, perturbed by unsteady effects.

Appendix

In this Appendix, (3.1) and (3.2) are derived. Because the way to derive each of the four equations is identical, we specify here only how we obtain the first result:

$$\mathscr{F}_t^{-1}\left(\frac{1}{\sqrt{-\mathrm{i}(\Omega+2)}}\right)=\frac{1}{2\pi}\int_{\mathbb{R}}\frac{\exp(-\mathrm{i}\Omega t)}{\sqrt{-\mathrm{i}(\Omega+2)}}\,\mathrm{d}\Omega. \tag{A 1}$$

By setting $\Omega'=\Omega+2$, we are led to

$$\mathscr{F}_t^{-1}\left(\frac{1}{\sqrt{-\mathrm{i}(\Omega+2)}}\right)=\frac{\exp(2\mathrm{i}t)}{2\pi}\int_{\mathbb{R}}\frac{\exp(-\mathrm{i}\Omega' t)}{\sqrt{-\mathrm{i}(\Omega')}}\,\mathrm{d}\Omega', \tag{A 2}$$

and this integral can be split in two parts

$$\int_{\mathbb{R}}\frac{\exp(-\mathrm{i}\Omega' t)}{\sqrt{-\mathrm{i}(\Omega')}}\,\mathrm{d}\Omega'=\int_{-\infty}^{0}\frac{\exp(-\mathrm{i}\Omega' t)}{\sqrt{-\mathrm{i}(\Omega')}}\,\mathrm{d}\Omega'+\int_{0}^{\infty}\frac{\exp(-\mathrm{i}\Omega' t)}{\sqrt{-\mathrm{i}(\Omega')}}\,\mathrm{d}\Omega'.$$

For the negative Ω', we can write

$$\int_{-\infty}^{0}\frac{\exp(-\mathrm{i}\Omega' t)}{\sqrt{-\mathrm{i}(\Omega')}}\,\mathrm{d}\Omega'=\int_{0}^{\infty}\left(\frac{\sqrt{2}}{2}-\mathrm{i}\frac{\sqrt{2}}{2}\right)\frac{\cos(\Omega' t)+\mathrm{i}\sin(\Omega' t)}{\sqrt{\Omega'}}\,\mathrm{d}\Omega',$$

whereas for the positive Ω', we have

$$\int_{0}^{\infty}\frac{\exp(-\mathrm{i}\Omega' t)}{\sqrt{-\mathrm{i}(\Omega')}}\,\mathrm{d}\Omega'=\int_{0}^{\infty}\left(\frac{\sqrt{2}}{2}+\mathrm{i}\frac{\sqrt{2}}{2}\right)\frac{\cos(\Omega' t)-\mathrm{i}\sin(\Omega' t)}{\sqrt{\Omega'}}\,\mathrm{d}\Omega'.$$

Finally,

$$\int_{\mathbb{R}}\frac{\exp(-\mathrm{i}\Omega' t)}{\sqrt{-\mathrm{i}(\Omega')}}\,\mathrm{d}\Omega'=\int_{0}^{\infty}\sqrt{2}\left(\frac{\cos(\Omega' t)+\sin(\Omega' t)}{\sqrt{\Omega'}}\right)\mathrm{d}\Omega'=\frac{2\sqrt{\pi}}{\sqrt{t}},$$

and substituting this last expression into (A 2) provides of (3.1*a*).

REFERENCES

Asmolov, E. & McLaughlin, J. B. 1999 The inertial lift on a oscillating sphere in a linear shear flow. *Intl J. Multiphase Flow* **183**, 199–218.

Candelier, F. & Angilella, J. R. 2006 Analytical investigation of the combined effect of fluid inertia and unsteadiness on low-*Re* particle centrifugation. *Phys. Rev.* E **73**, 047301.

Candelier, F. & Souhar, M. 2007 Time-dependent lift force acting on a particle moving arbitrarily in a pure shear flow, at small Reynolds number *Phys. Rev.* E **76**, 067301.

Candelier, F., Angilella, J.-R. & Souhar, M. 2004 On the effect of the Boussinesq–Basset force on the radial migration of a Stokes particle in a vortex. *Phys. Fluids* **16**(5), 1765–1776.

Candelier, F., Angilella, J.-R. & Souhar, M. 2005 On the effect of inertia and history forces on the slow motion of a spherical solid or gaseous inclusion in a solid-body rotation flow. *J. Fluid. Mech.* **545**, 113–139.

Childress, S. 1964 The slow motion of a sphere in a rotating, viscous fluid. *J. Fluid Mech.* **20**, 305–314.

Gotoh, T. 1990 The Brownian motion in a rotating flow. *J. Stat. Phys.* **59**, 371–390.

Herron, I. H., Davis, S. & Bretherton, F. P. 1975 On the sedimentation of a sphere in a centrifuge. *J. Fluid Mech.* **68**, 209–234.

Landau, L. & Lifchitz, E. 1989 *Physique Théorique, vol. 6, Mécanique des Fluides*, pp. 127–129. Mir.

Maxworthy, T. 1965 An experimental determination of the slow motion of a sphere in a rotating viscous fluid. *J. Fluid Mech.* **23**, 373–384.

Miyazaki, K. 1995 Dependence of the friction tensor on the rotation of a frame of reference. *Physica* A **222**, 2489–260.

Miyazaki, K., Bedeaux, D. & Bonnet Avalos, J. 1995 Drag on a sphere in a slow shear flow. *J. Fluid Mech.* **296**, 373–390.

van Nierop, E. A., Luther, S., Bluemink, J. J., Magnaudet, J., Prosperetti, A. & Lohse, D. 2007 Drag and lift forces on bubbles in a rotating flow. *J. Fluid Mech.* **571**, 439–454.

Saffman, P. G. 1965 The lift on a small sphere in a slow shear flow. *J. Fluid Mech.* **22**, 385–400; and Corrigendum, **31**, 1968, 624.

Wakaba, L. & Balachandar, S. 2005 History force on a sphere in a weak linear shear flow. *Intl J. Multiphase Flow.* **31**, 996–1014.